Pterygomaxillary Region in Implantology: A Topographic and Radiological Study

Abstract

Background
Implant rehabilitation of the atrophic posterior maxilla remains challenging due to sinus pneumatization and poor bone density. Pterygo-maxillary implants represent an anatomically feasible option for posterior maxillary rehabilitation; however, this study evaluates their virtual planning characteristics only, without assessing clinical outcomes.

Objectives
This study aimed to assess the three-dimensional characteristics of the pterygomaxillary region relevant for implant placement, and propose a standardized CBCT-based diagnostic protocol to optimize individualized implant planning.

Methods
Twenty CBCT scans were evaluated bilaterally (40 potential implant sites). Bone density, anatomical dimensions, implant angulations, and virtual implant positioning were analyzed. A novel proposed reference plane, the Maxillary Plane, was developed to provide a consistent virtual framework for analyzing implant trajectories, but does not assess clinical performance.

Results
34 virtual pterygo-maxillary implants were successfully planned. Implant lengths ranged between 11–15 mm and diameters between 3.3–3.8 mm. Bone density was consistently higher in the pterygoid lamina compared to the maxillary tuberosity. Implant angulation showed substantial interindividual variability.

Conclusions
The anatomical variability of the pterygomaxillary region requires individualized CBCT analysis. The proposed Maxillary Plane is a theoretically applicable methodological innovation for standardized implant angulation assessment. Pterygomaxillary implants represent a predictable and minimally invasive alternative for posterior maxillary rehabilitation in cases of severe atrophy.

Authors

Michele Manacorda[1]
Francesco Ferrini[1]
Luisa Paternoster[2]*
Arianna Rodriguez y Baena[2]
Raffaele Vinci[3]

1
DDS, Dental School, Vita-Salute San Raffaele University, Milan, Italy

2
DDS, Dental School, Vita-Salute San Raffaele University, Milan, Italy

3
MD MFS, Full Professor and Director of post-graduate School in Oral Surgery, Vita-Salute San Raffaele University, Milan, Italy

*Corresponding Author

Keywords

Pterygoid implant, tuberosity implant, pterygomaxillary region, CBCT planning, implant angulation, posterior maxilla, bone atrophy.

DOI

10.23805/JO.2026.802

INTRODUCTION

Rehabilitation of the edentulous posterior maxilla remains a complex task due to anatomical limitations such as maxillary sinus pneumatization and low-density cancellous bone (1-2). Conventional reconstructive procedures—including sinus lift, guided bone regeneration (GBR), and zygomatic implants—can address these limitations but are associated with increased morbidity, cost, and treatment duration (3).
Tuberosity implants have been introduced as an alternative for avoiding grafting procedures; however, the tuberosity often contains type III–IV bone, reducing primary stability. To overcome this, Tulasne introduced the concept of pterygomaxillary implants, in which the implant is inserted through the tuberosity and anchored into the cortical bone of the pterygoid or pyramidal processes (4).
Engagement of the pterygoid plate provides increased primary stability, essential for favorable osseointegration and reduced prosthodontic cantilever forces (5-6-7).
Despite the growing popularity of this technique, anatomical variability and limited literature continue to generate uncertainty regarding implant dimensions, angulations, and safe surgical corridors (8). The present study addresses these gaps through a comprehensive radiological evaluation.

MATERIALS AND METHODS

Study design

A retrospective cross-sectional radiographic study was conducted at Vita-Salute San Raffaele University (Milan, Italy). Twenty CBCT scans were evaluated bilaterally (40 sides). Sites were classified for feasibility of tuberosity-only versus tuberosity with pterygoid anchorage implants or excluded for bone deficiency. This paper and the related research are based upon descriptive statistical analyses. No inferential statistical testing was performed, and the reported mean ± SD values are intended only to summarize anatomical variability within the sample.

Participants

Patients undergoing CBCT from December 2023 to January 2024 were screened.

Inclusion criteria

- Edentulous maxilla from bicuspid to posterior region
- Severe atrophy (residual bone height < 5 mm under sinus floor)

Exclusion criteria

- Radiopaque/radiolucent lesions
- Impacted teeth or existing implants in the region

Informed consent was obtained for all CBCT scans.

Imaging Acquisition

- Device: MyRay X9 Pro (Cefla SC, Italy)
- FOV: 12 × 8 cm
- Parameters: 90 kV, 10 mA, 16 s
- Voxel size: 0.2 mm

DICOM files were analyzed using RealGuide 5.4.2 (3Diemme, Italy).

Virtual Implant Planning

A highly experienced specialist evaluated:

- Bone density (GS scale)
- Buccopalatal and mesiodistal ridge width
- Anatomical relations with sinus, pterygoid plate, and palatine canal
- Implant angulations relative to newly defined reference plane

Placement criteria

- Minimum 2 mm from alveolar and basal cortical boundaries
- Apex no more than 1 mm beyond medial pterygoid wall
- Avoidance of sinus mucosa perforation
- Respect for palatine neurovascular structures

Analysis of the data and virtual implant positioning

An expert investigator provided all radiological measurements of the imported CBCT and virtually inserted implant phantoms in pterygo-maxillary region (Winsix TTi implants, Biosafin, Ancona, Italy).
The criteria taken into consideration were the following: height, width and bone density in pterygo-maxillary region of the edentulous and atrophic patients.
To assess intra-operator reliability of the radiological measurements, a single experienced operator re-evaluated a subset of CBCT scans (n = 20) after a time interval of 7 days. Linear and angular measurements were repeated following the same diagnostic protocol. Intra-operator agreement was quantified using the intraclass correlation coefficient (ICC) with a two-way mixed-effects model, absolute agreement, single measurement (ICC(3,1)).
With the data obtained from each case, an individual implant planning has been made through the positioning of virtual implants in the pterygo-maxillary region.
Each implant has been placed with a distance of at least 2 mm from the vestibular and palatal bone margins and not more than 1 mm out of the pterygoid plate.
The apex of tuberosity implants with pterygoid anchorage should not exceed one millimeter beyond the medial wall of the pterygoid process, in correspondence to the pterygo-maxillary junction. The limit of 1 mm beyond the medial wall represents

a conservative planning threshold specific to our virtual workflow, adopted to avoid overestimating bone engagement in a non-clinical simulation. This threshold is not intended as a clinical recommendation nor a universally applicable guideline.
For every planned implant we studied length and depth of the fixture and its spatial position: mesio-distal tilting, angular deviation from the axial position.

Anatomical landmarks
An understanding of the anatomy of the pterygo-palato-maxillary region is needed to fully comprehend this technique and the risks associated with it.
The posterior maxilla can be defined as the pterygo-palato-maxillary region because it is composed of several bone structures: maxillary tuberosity, pyramidal process of palatine bone and pterygoid plates of the sphenoid bone (4-5).
The fusion between the previously mentioned bone structures forms a highly interesting area from a mechanical point of view in implantology although tuberal poor bone quality (4).
Maxillary tuberosity internally articulates with the pyramidal process of the palatine bone and posteriorly it joins the pterygoid process of the sphenoid bone forming the pterygomaxillary junction which is crossed by the pterygoid canal.
The lower portion of pterygoid process is connected to the maxillary tuberosity forming the pterygo-maxillary junction. The variability of this anatomical structure is high: it has been demonstrated that this junction can remain as a fissure separating the maxillary tuberosity from the pterygoid plate (88% of the cases) or it can be a synostosis fusing the two bones together (12%) (6).
Knowing the height of this junction is fundamental in order to localize the pterygopalatine fissure which is located lateral and under the pterygopalatine fossa, an important neurovascular cross-road (9-15).

Radiological landmarks

An accurate study of CBCT can help the clinician to plan the implant insertion in a poor density tuberal bone but reaching an area with D1/D2 bone, emerging crestal to the first, second molar position.
Given that orthopantomography is not sufficient for planning the insertion of a pterygo-maxillary implant, a CBCT scan is required to determine the length, width and angle of each individual implant fixture. In the axial projection, it is possible to determine the width of the maxillary tuber and, scrolling through the images cranially, it is possible to see the extension of the sinus, the posterior border of the tuber maxillae, up to the pterygoid junction. Along the palatal side, it is possible to locate the path of the greater palatine artery and its emergence on the palatal vault.
Specific software provides us with the density of the cancellous and cortical bone to plan the diameter of the bone drilling burs to achieve good primary stability.
The axial view is used as a precise and individual reference to select the panoramic view.
The curve must be selected starting from beyond the pterygoid plates in order to view the entire anatomical region of interest (Fig. 1).
The curve must be positioned exactly halfway between the two pterygoid plates to avoid false information in the panorex image. At this point, we obtain a pseudo-panoramic image that will be orthogonal to our reference plane, i.e. the maxilla.
On the panorex image, we check the extension of the maxillary tuberosity and the topographical anatomy of the maxillary sinus at the crestal and tuberous levels.
Then, a cutting plane must be selected to define a cross-section of the area of interest. The cross section is defined as a parasagittal section orthogonal to the panoramic curve selected at that point. This allows us to visualise the vestibulo-palatal thickness of the bone, the thickness of the cortices, the relationships with anatomical structures of interest such as arteries and nerves, and the available bone height.
In the latest radiological diagnostic software equipped with the multiplanar visualisation function, we are able to choose a cross section that is not orthogonal to the panoramic curve, but rather inclined, in order to better visualize the real bone anatomy for a tilted implant.
Once the ideal cross section has been obtained, virtual implant planning can take place.
This cross-sectional view is the right image for

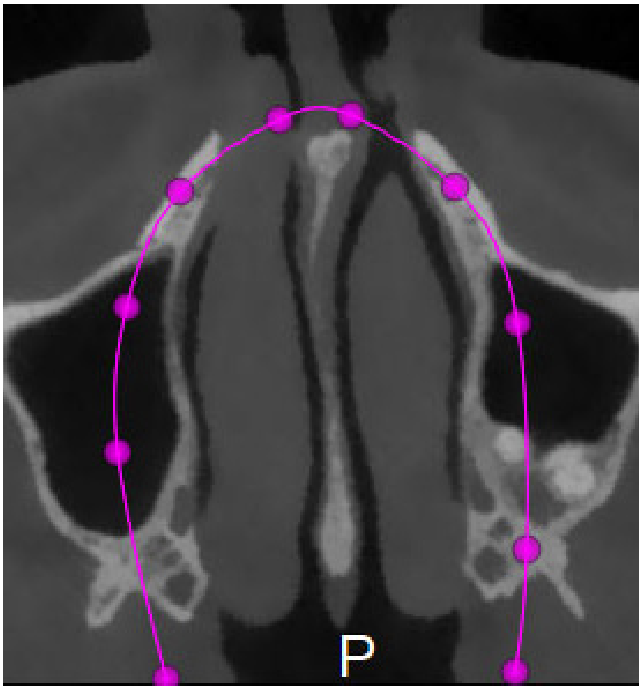

Fig. 1 Design for creating a correct panorex view. It's possible to appreciate pterygoid plates.

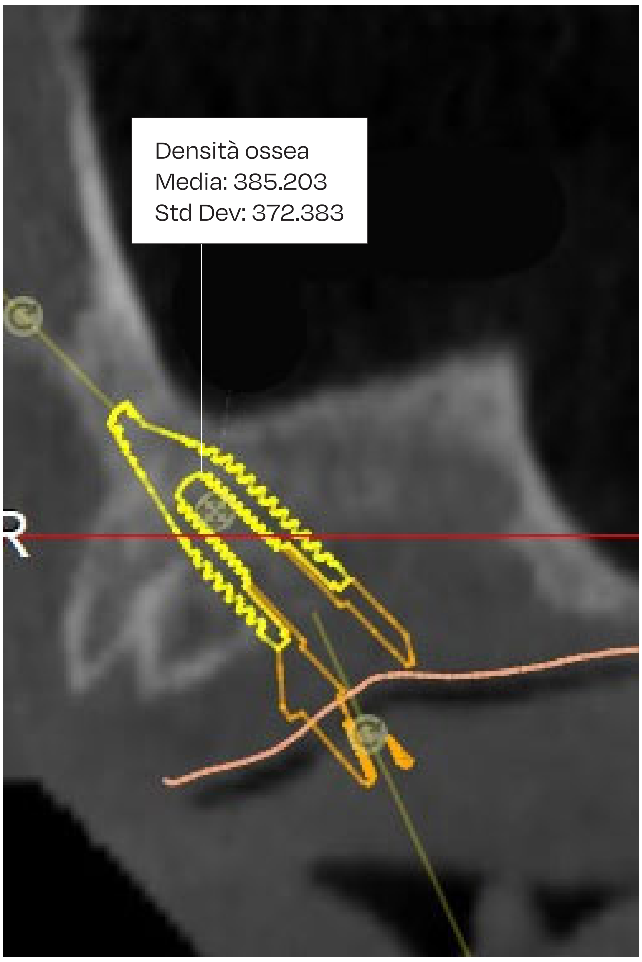

Fig. 2 3D planned implant insertion in cross and panorex view. The implant is positioned respecting anatomical structures such as maxillary sinus and palatal artery

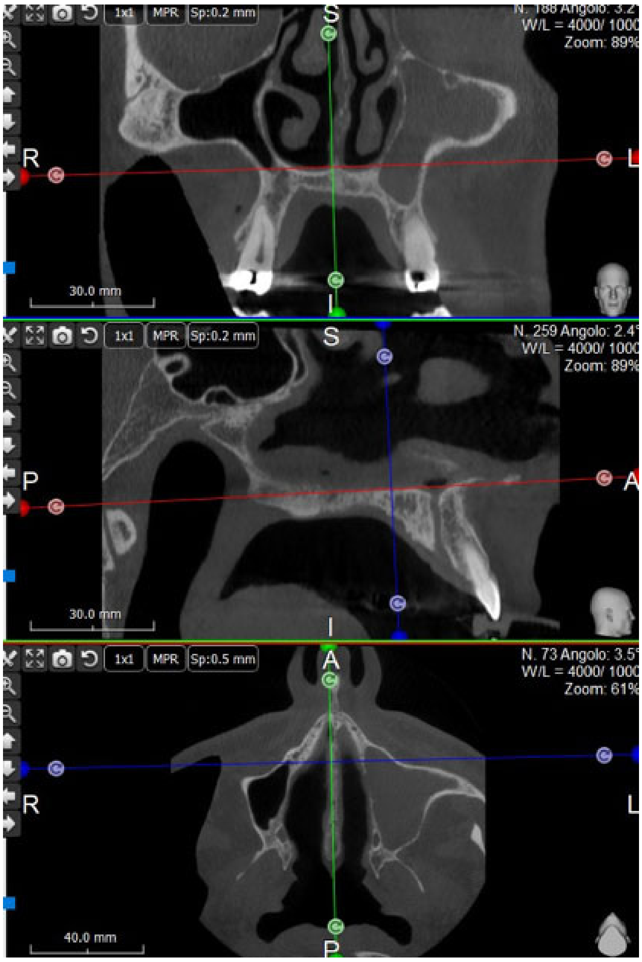

Fig. 3 Tracking of SNA and SNP line in CBCT axial, sagittal and coronal view.

planning the implant site, also evaluating the bone quality around the implant surface (Fig. 2).
Accurate study of CBCT images and virtual positioning of the implant prior to surgery can assist the surgeon in preparing a generally sensitive-dependent and semi-blind implant site, which is potentially at high risk of invasion of vital structures (16).

Virtual implants insertion in surgical planning

The decision to perform scans using CBCT rather than spiral CT is based on the significant reduction in the radiation doses to which the patient is exposed, also achieved by reducing the FOV (17). This limits the visualization of the entire facial skeleton and does not allow the tracking of Frankfurt plane, usually used as a reference plane to calculate implant insertion angulation (18).
In this study, we propose the maxillary plane as a reference plane, defined in the CBCT median sagittal view as the plane passing through the SNA (anterior nasal spine) and SNP (posterior nasal spine) points and parallel to OR1 and OR2, i.e. the right lower orbital rim and the left lower orbital rim (Fig. 2-3).
Prior to CBCT acquisition, scout images were used to adjust the FOV so that the anterior nasal spine (SNA), posterior nasal spine (SNP), and both infraorbital rims (OR1 and OR2) were included in the volume when angulation analysis was needed. Because visibility of infraorbital rims is FOV-dependent, a fixed FOV is not sufficient for reproducibility; instead, the radiographer must adapt the FOV to the patient's anatomy as visualized in the scout view. If one infraorbital rim was not adequately captured, the scan was considered unsuitable for constructing the Maxillary Plane. If neither OR1 nor OR2 was visible, angulation analysis was not performed. These fallback criteria ensure conceptual reproducibility independent of software-specific visualization.
This choice allows for unambiguous measurement of the implant design (Fig. 4).
The importance of these points lies in the fact that they are always fixed, easily recognized in CBCT and they cannot be modified by maxillary bone atrophy, such as the occlusal plane (19-20).

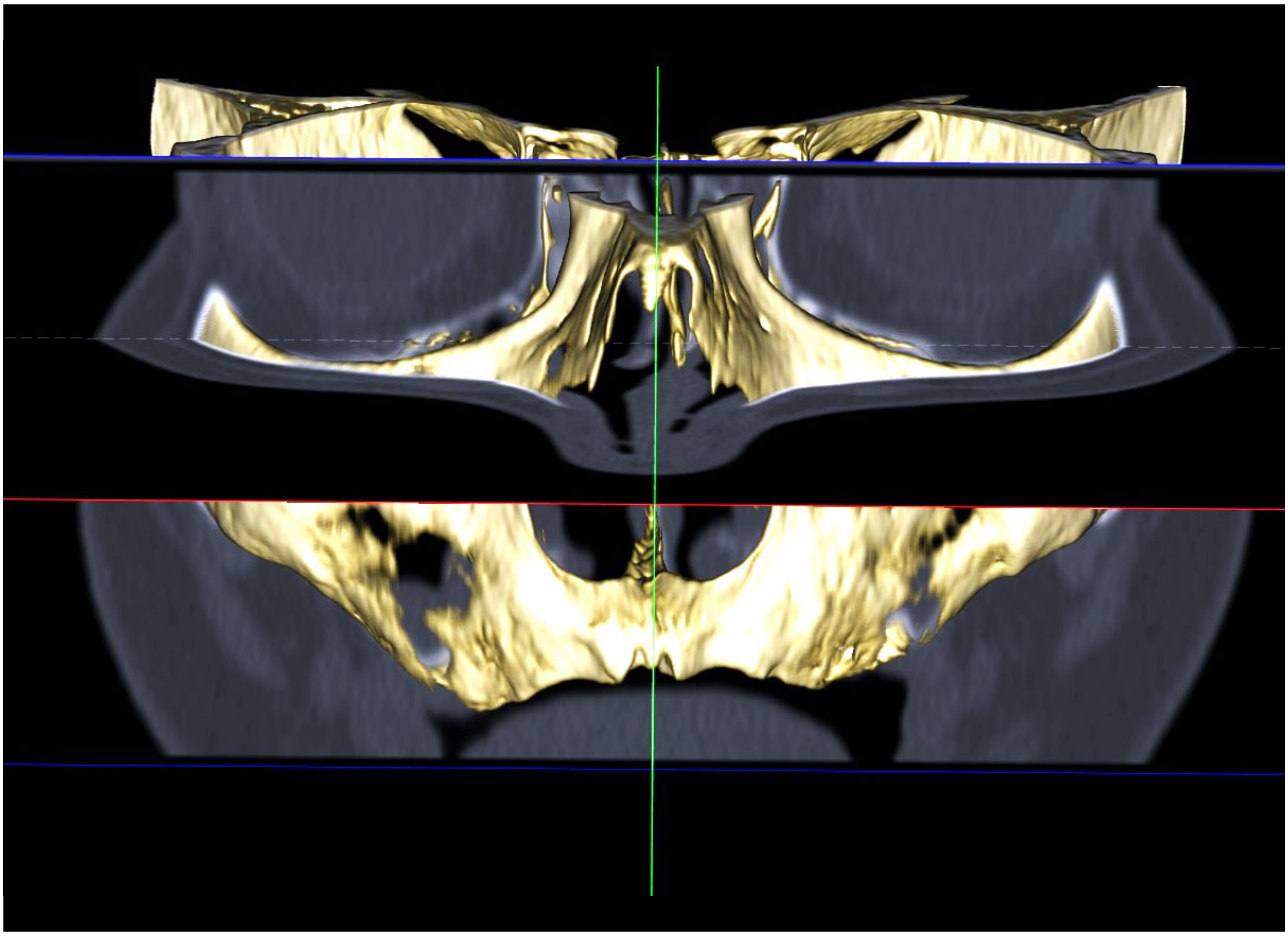

Fig. 4 Tracking of the maxillary plane parallel to SNA and SNP line an d crossing OR1 and OR2.

This method of selecting the reference plane individually for each CBCT allows to compensate for any alterations in the correct positioning of the patient during the X-ray examination, making the virtual positioning of the implant in relation to the plane in question unequivocal and repeatable (Fig. 5).

RESULTS

A total of 20 patients were included in the study, providing 40 pterygoid sites potentially eligible for pterygoid implant placement. Of these, 6 sites were excluded according to predefined exclusion criteria, resulting in a final sample of 34 pterygoid sites from 20 patients. Since each patient could contribute bilateral pterygoid sites (right and left), observations were not considered statistically independent. Bilateral sites within the same patient share anatomical and clinical characteristics, resulting in within-patient correlation. To account for this hierarchical data structure (sites nested within patients), analyses of continuous outcomes were performed using linear mixed-effects models including a random intercept for patient (patient as the clustering unit). The side (right vs. left) was included in the model as a fixed effect to evaluate potential lateral differences (Tab. 1).

The table below reports:

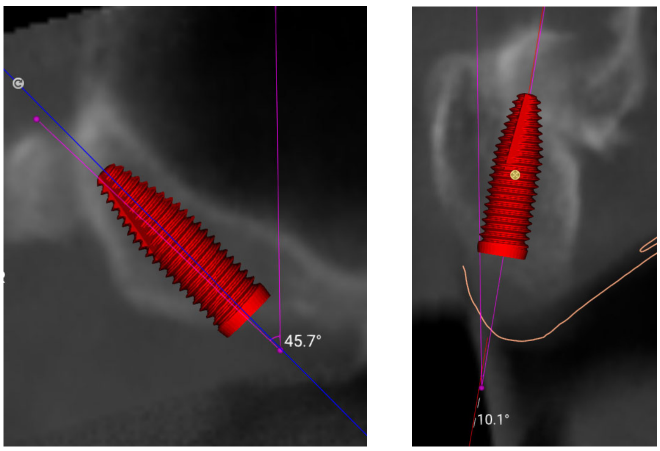

Fig. 5 Virtual implant planning in panorex and parasagittal section showing the mesio-distal and vestibulo-palatal inclination of the fixture referred to maxillary plane.

Cbct	Side	Bd (Gs)	I M-D (°)	I V-P (°)	Id (mm)
1	R	Insuficient Bone Quantity	X	X	X
1	L	703.5	33.0°	17.9°	3.3 x 11 mm
2	R	575	23.8°	8.1°	3.8 x 15 mm
2	L	Tuberal Implant	X	X	X
3	R	255	35.7°	19.4°	3.8 x 11 mm
3	L	280	35.6°	2.2°	3.8 x 11 mm
4	R	456	40.6°	5.0°	3.3 x 11 mm
4	L	222	26.2°	16.3°	3.3 x 11 mm
5	R	468	37.5°	9.2°	3.8 x 15 mm
5	L	446	37.8°	10.8°	3.8 x 15 mm
6	R	Insuficient Bone Quantity	X	X	X
6	L	341	32.4°	23.2°	3.8 x 13 mm
7	R	243	33.1°	2.6°	3.8 x 15 mm
7	L	Tuberal Implant	X	X	X
8	R	450	28.5°	8.4°	3.8 x 13 mm
8	L	412	29.3°	15.4°	3.8 x 13 mm
9	R	385	44.3°	3.9°	3.8 x 11 mm
9	L	258	44.8°	12.3°	3.8 x 11 mm
10	R	377	33.6°	-7.4°	3.3 x 11 mm
10	L	550	28.6°	-4.5°	3.8 x 13 mm
11	R	352	37.5°	14.5°	3.8 x 15 mm
11	L	280	16.3°	9.1°	3.8 x 15 mm
12	R	466	25.8°	-5.9°	3.8 x 11 mm
12	L	445	35.2°	-4.5°	3.8 x 11 mm
13	R	Tuberal Implant	X	X	X
13	L	441	45.0°	2.1°	3.8 x 13 mm
14	R	253	45.0°	-1.8°	3.8 x 11 mm
14	L	Tuberal Implant	X	X	X
15	R	355	27.4°	21.5°	3.8 x 15 mm
15	L	260	19°	15.9°	3.8 x 15 mm
16	R	489	25.4°	15.9°	3.8 x 13 mm
16	L	456	33.5°	14.6°	3.8 x 11 mm
17	R	290	42.9°	18.0°	3.3 x 11 mm
17	L	377	35.0°	23.2°	3.3 x 13 mm
18	R	440	28.9°	11.2°	3.8 x 13 mm
18	L	349	37.0°	12.5°	3.8 x 13 mm
19	R	455	28.6°	13.4°	3.8 x 13 mm
19	L	244	16.0°	20.4°	3.3 x 13 mm
20	R	330	38.0°	15.6°	3.8 x 11 mm
20	L	514	40.3°	16.6°	3.8 x 15 mm

Tab. 1 Summary of bone density, mesiodistal and buccopalatal angulations and implant dimensions for left(L) and right (R) side of each patient's CBCT(from 1 to 20).

- BD: bone density
- I M–D: mesio–distal angulation
- I V–P: vestibulo–palatal angulation
- Implant dimension (ID): implant length and diameter
- GS: Gray-Scale values provided by the Real Guide

5.4.2 (3Diemme) software

Since CBCT diagnostic software does not employ a standardized density scale equivalent to Hounsfield Units used in CT imaging, bone density values were expressed using the Gray-Scale (GS).

As CBCT gray-scale units are device- and software-dependent and do not correspond to calibrated Hounsfield Units, density values in this study were used exclusively for within-study comparisons between anatomical regions. No absolute quantification of bone density and no cross-study comparability are implied. GS measurements were interpreted as relative differences within our sample, not as absolute material density. Bone density, mesiodistal and buccopalatal angulations, and implant dimensions for each case are summarized in Table 1.

The analysis of the 34 virtually planned pterygoid implants showed a mean bone density (BD) of 388.75 ± 111.57 (Gray-scale).

The mean mesio-distal inclination (IM-D) was 32.99° ± 7.82°, while the vestibulo-palatal inclination (IV-P) showed a mean value of 10.44° ± 8.60°.

Most of inclinations were vestibulo-palatal, but in cases of extreme atrophy, the inclination of the implants is palatal-vestibular, as can be seen from the negative values shown in the table.

ICC values demonstrated good intra-operator reliability for all measurements, as reported below:

- BD: ICC = 0.82 (95% CI: 0.74–0.89)
- IM-D: ICC = 0.84 (95% CI: 0.76–0.90)
- IV-P: ICC = 0.79 (95% CI: 0.68–0.87)

These values indicate good intra-operator repeatability but do not establish inter-operator reproducibility.

Radiological diagnostic software used for the interpretation of CBCT scans currently does not share a standardized reference unit for bone density measurement, unlike conventional CT imaging, which relies on Hounsfield Units (HU). The Real Guide 5.4.2 (3Diemme, Cantù, Italy) software, used in this study, allows the assessment of bone density using the Gray-Scale (GS). The analysis of GS-derived density values showed that the pterygoid plate region consistently presented higher gray-scale values than the maxillary tuberosity. These values represent relative intra-study differences only, reflecting anatomical variation within our sample. Because GS units are device-dependent and non-standardized, no absolute interpretation of bone density and no cross-study comparisons were performed (21). The results section includes a table reporting the analysis of 20 CBCT scans, yielding 34 virtually planned pterygoid implants (6 sites were excluded because they were either tuberal – adequate bone to implant contact- or exhibited insufficient bone volume to allow implant planning). The values obtained for each scan are presented in detail. These findings were subsequently compared to the existing literature to highlight similarities, discrepancies, and specific aspects related to the technique adopted in the present study. As this study was descriptive, no hypothesis testing or inferential statistics were performed. Reported values represent summary measures intended to describe anatomical variation within the sample.

DISCUSSION

Rehabilitation of the edentulous posterior maxilla in cases of severe bone atrophy represents a significant challenge, even for experienced clinicians. The surgical technique involving the placement of tuberous implants anchored to the pterygoid process of the sphenoid bone follows the same fundamental principles as conventional implant surgery and may be considered relatively straightforward. The procedure does not require bone grafting, is associated with reduced morbidity, lower overall treatment costs, and shorter healing periods (22). From a prosthetic standpoint, rehabilitation supported by pterygoid-anchored implants offers the crucial advantage of eliminating long distal cantilevers, as implant emergence occurs in the maxillary arch at the level of the second molar (23).

Several authors emphasize the need to differentiate true pterygo-maxillary implants from tuberal implants, as the latter—by definition—do not engage the pterygoid lamina (24-25). This differentiation is clinically significant because these bone structures have different anatomical and biomechanical properties, which may influence implant survival. Engagement of cortical bone is known to enhance primary stability and, consequently, the likelihood of successful osseointegration (26-27-28-29).

A second point of debate concerns implant length required to achieve pterygoid plate engagement. Some studies suggest a minimum length of 13 mm. Rodríguez, author of multiple articles on the topic, reports average implant lengths of 18 mm in his most recent work, while earlier studies document successful virtual placement with lengths of 13, 15, and 18 mm depending on anatomy (30-31-32). Balshi, in a large series of 992 implants, concluded that implants measuring 15–18 mm exhibit higher long-term survival, given their ability to engage cortical bone between the medial and lateral pterygoid plates, improving both primary and secondary stability (33). A recent review by Bidra recommends implant lengths between 15–20 mm and suggests that penetration of the pterygoid fossa by approximately 2 mm may be necessary (34-35). In contrast, Uchida advises against implants longer than 15 mm due to the risk posed to the delicate anatomical structures located immediately beyond the pterygoid lamina (36).

The results of the present study demonstrate that there is no universally applicable implant length for this region. Each case must be evaluated individually using CBCT imaging before surgery. Length is determined by the amount of residual tuberosity bone, the chosen angulation, and the position of the pterygoid plate, which varies greatly across individuals. In our series, virtual placement of implants as short as 11 mm was necessary due to pronounced atrophy. These findings are not merely theoretical: the patient detailed in the table underwent actual surgery, and the implant placed (3.3 × 11 mm) fully corresponded to the virtual plan. Therefore, shorter implants should not be dismissed outright; depending on individual anatomy, even relatively short implants may achieve stable engagement with the pterygoid plate.

A similar rationale applies to implant diameter. Few authors address this variable, but those who do report average diameters between 3.75–4.0 mm (30-31-32-33). In our clinical experience, implant diameter should ensure adequate bone–implant contact; however, reduced bone volume may necessitate the use of narrower implants (e.g., 3.3 mm). Current literature does not provide sufficient evidence to suggest that these narrower implants have inferior outcomes.

Another major controversy concerns the angulation required for correct pterygoid implant placement, particularly in relation to the reference plane used for measurement (37). Some authors employ the Frankfurt Horizontal Plane (Porion–Orbitale), suggesting ideal angles ranging from 45° to 70° (Graves; Rodríguez) (26-31-32-33), although such verticalized angulation may lead to non-axial transmission of occlusal forces, compromising prosthetic longevity. Moreover, excessive lingual inclination has been associated with increased risk of damaging the greater palatine canal (Suzuki et al., 2016; Taniguchi et al., 2024) (38-39).

Rodríguez reports mesio-distal inclinations around 74° and vestibulo-palatal inclinations around 81° relative to the Frankfurt plane, values similar to those documented by Uchida.(29-30-31-35) However, this plane is difficult to reproduce consistently in CBCT scans with a reduced field of view, as the Porion–Orbitale landmarks may not be visible. Conversely, Balaji and Bidra use the “maxillary plane” as a reference, reporting inclinations of 45–50° and 45–60°, respectively, but do not clearly define this plane, making replication difficult during digital planning (35-39).

For these reasons, we propose a new definition of the maxillary reference plane suitable for use in CBCT-based planning, as described in detail in the Materials and Methods. This individualized plane selection compensates for variations in patient positioning during radiographic acquisition and ensures consistency in virtual planning across all cases.

The definition of the Maxillary Plane requires visualization of SNA, SNP, and the infraorbital rims. Because their visibility is directly dependent on the acquisition protocol, especially the field of view, reproducibility requires proper FOV selection based on scout images, rather than assuming a fixed FOV is sufficient. Although all landmarks were visible in our dataset, this was the result of deliberate FOV adjustment and cannot be generalized to devices or protocols where the scout view is not used to guide positioning.

Regarding implant angulation, another controversy concerns whether to measure only the mesio-distal component or to include the vestibulo-palatal component as well. Although some studies consider only one plane, we believe both must be evaluated due to the proximity of critical anatomical structures—such as the greater palatine artery and nerve—which emerge only a few millimeters from the pterygoid engagement zone. Inadequate vestibulo-palatal angulation could significantly increase the risk of injury.

Bone density in the maxillary tuberosity and pterygoid lamina is rarely reported in the literature. Rodríguez describes the pterygoid lamina as being 139% denser than tuberosity bone (30), while Salinas-Goodier reports an 87% difference. Previous studies classify tuberosity bone as type III or IV (41), with Jaffin and Berman reporting a 35% failure rate for implants in type IV bone versus only 3% in denser bone types (42). Thus, achieving primary stability in the atrophic posterior maxilla is strongly dependent on local bone density.

Preoperative CBCT evaluation provides valuable information on bone density through Grays-Scale values. Therefore, personalized assessment of both tuberosity and pterygoid bone is essential to determine implant dimensions and optimize surgical outcomes. For the purposes of this study, GS-derived density measurements were interpreted only as relative internal indicators of the anatomical variability between the tuberosity and the pterygoid plate. No absolute values or cross-study comparisons were inferred from gray-scale data.

Use of an implant motor with real-time torque feedback further enhances safety by identifying cortical engagement and preventing over-penetration into delicate anatomical structures.

Although CBCT software lacks a standardized density scale equivalent to Hounsfield Units used in CT, the Real Guide 5.4.2 (3Diemme) platform provides density assessment through the Gray-Scale.

Complications associated with pterygoid implant placement are minimal when the technique is performed correctly. The literature and our clinical experience suggest that the main challenges involve anatomical expertise and the surgical learning curve. According to the authors, pterygoid implants should be used only when strictly necessary, as the least invasive treatment option should always be preferred when clinically feasible. When the tuberosity presents sufficient bone volume and density to provide adequate primary stability, tuberal-only implants should be prioritized.

As measurements were performed by a single operator, inter-operator reproducibility was not assessed, and the findings should be interpreted as reflecting intra-operator consistency rather than general reproducibility.

The present findings describe the anatomical feasibility of pterygoid implant positioning in a virtual environment. Because no surgical procedures or follow-up were performed, no conclusions regarding clinical reliability, predictability, or treatment success can be drawn.

To reproduce the planned inclination during clinical placement, the use of a surgical guide is strongly recommended. Based on our experience, the guide should be used for the pilot drill, while subsequent preparation may be completed freehand to allow the surgeon to confirm tactile feedback, cortical engagement, and implant stability.

The results reflect virtual planning only and cannot be extrapolated to actual surgical performance, implant survival, complication rates, or long-term outcomes.

Conclusions

As demonstrated by the results, a total of 34 pterygo-maxillary implants were virtually positioned. As expected from anatomical evidence, bone density is markedly higher in the pterygoid lamina than in the maxillary tuberosity. For the purposes of this study, the average bone density surrounding the implant fixture was used as the reference parameter, as this value most accurately reflects the ability of the implant to achieve adequate primary stability and, consequently, successful osseointegration.

Both mesio–distal and vestibulo–palatal angulations, calculated relative to the maxillary reference plane defined during planning, showed a high degree of variability across cases. The smallest mesio–distal inclination recorded was 16.3°, while the greatest reached 45°. For the vestibulo–palatal inclination, values ranged from −7.4° to 23.2°, confirming that angulation is strongly influenced by individual anatomical differences.

Implant lengths were selected based on available bone, resulting in fixtures measuring 11 mm, 13 mm, and 15 mm. Specifically, 11 implants measured 11 mm, 5 implants measured 13 mm, and 6 implants measured 15 mm. The standard diameter used in this study was 3.8 mm; however, in four cases, implants with a 3.3 mm diameter were necessary due to severe bone atrophy.

This substantial variability in density, angulation, and implant dimensions underscores the absolute necessity of individualized preoperative CBCT assessment for every patient. Only through detailed anatomical and radiographic analysis can clinicians ensure accurate planning, optimal implant choice, safe surgical execution, and long-term clinical success.

A major limitation of this study is that all analyses were descriptive. While this design is appropriate for anatomical characterization, it does not allow conclusions regarding predictive factors or causal relationships. Future studies with larger sample sizes and inferential statistical approaches are needed to determine whether the measured variables influence clinical outcomes.

Because the analysis is limited to virtual simulation without clinical follow-up, no statements regarding clinical predictability, reliability, or treatment success can be made.For this reason and because it's a blind surgery , we suggest clinicians to use an implant surgical template in order to be as precise as possible during implant placement.

However, further studies with a larger number of patients and measurements taken by more than a single operator are needed to confirm the results obtained.

REFERENCES

1. Aparicio C, Perales P, Rangert B. Tilted implants as an alternative to maxillary sinus grafting: a clinical, radiologic and periotest study. Clin Implant Dent Relat Res. 2001;3(1):39-49.

2. Tolstunov L, Thai D, Arellano L.Implant-guided volumetric analysis of edentulous maxillary bone with cone-beam computerized tomography scan. Maxillary sinus pneumatization classification. J Oral Implantol. 2012;38(4):377-90.

3. Araujo RZ, Santiago Júnior JF, Cardoso CL, Benites Condezo AF, Moreira Júnior R, Curi MM. Clinical outcomes of pterygoid implants: Systematic review and meta-analysis. J Craniomaxillofac Surg. 2019;47:651–60.

4. Tulasne JF. Osseointegrated fixtures in the pterygoid region. In: Worthington P, Branemark PI, editors. Advanced Osseointegration surgery: applications in the Maxillofacial region. Chicago, III: Quintessence Publishing; 1992. p. 182–8.

5. Zhang Q, Abdelrehem A, Qu XZ, Zhang CP, Ong HS. Radiographic analysis of critical anatomical structures for pterygoid implant placement in Chinese patients with a severely atrophied maxilla. Int J Oral Maxillofac Surg. 2023;52:998–1004.

6. du Toit DF, Nortje C. The maxillae: integrated and applied anatomy relevant to dentistry. SADJ. 2003;58:325–30.

7. Testori T, Clauser T, Rapani A, Artzi Z, Avila-Ortiz G, Barootchi S, Bressan E, Chiapasco M, Cordaro L, Decker A, De Stavola L, Di Stefano DA, Felice P, Fontana F, Grusovin MG, Jensen OT, Le BT, Lombardi T, Misch C, Pikos M, Pistilli R, Ronda M, Saleh MH, Schwartz-Arad D, Simion M, Taschieri S, Toffler M, Tozum TF, Valentini P, Vinci R, Wallace SS, Wang HL, Wen SC, Yin S, Zucchelli G, Zuffetti F, Stacchi C. Indications for implant-supported rehabilitation of the posterior atrophic maxilla: A multidisciplinary consensus among experts in the field utilising the modified Delphi method. Int J Oral Implantol (Berl). 2024 Mar 19;17(1):89-100. PMID: 38501401.

8. Bornstein MM, Scarfe WC, Vaughn VM, Jacobs R. Cone beam computed tomography in implant dentistry: a systematic review focusing on guidelines, indications, and radiation dose risks. Int J Oral Maxillofac Implants. 2014;29 Suppl:55-77. doi: 10.11607/jomi.2014suppl.g1.4. PMID: 24660190.

9. Ulm C, Solar P, Matejka M, Watzek G. The atrophy of the edentulous and partially dentate alveolar process of the maxillae (article in German). Implantologie. 1993;4:305–14.

10. Chrcanovic BR, Abreu MH, Custodio AL. A morphometric analysis of supraorbital and infraorbital foramina relative to surgical landmarks. Surg Radiol Anat. 2011;33:329–35.

11. Traxler H, Windisch A, Geyerhofer U, Surd R, Solar P, Firbas W. Arterial blood supply of the maxillary sinus. Clin Anat. 1999; 12:417–21.

12. Ten Bruggenkate CM, Kraaijenhagen HA, van der Kwast WA, Krekeler G, Oosterbeek HS. Autogenous maxillary bone grafts in conjunc- tion with placement of ITI endosseous implants. A preliminary report. Int J Oral Maxillofac Surg.1992;21:81–4.

13. Murakami G, Ohtsuka K, Sato I, Moriyama H, Shimada K, Tomita H. The superior alveolar nerves: their topographical relationship and distribution to the maxillary sinus in human adults. Okajimas Folia Anat Jpn. 1994;70:319–28.

14. Heasman PA. Clinical anatomy of the superior alveolar nerves. Br J Oral Maxillofac Surg. 1984;22:439–47.

15. Moretto EP, Silva GH, Toldeo Filho JL, Andreo JC, Navarro Rde L, Navarro JA. Surgical anatomy of the maxillary nerve in the zygo- matic region. J Appl Oral Sci. 2005;13:167–70.

16. Vrielinck L, Politis C, Schepers S, Pauwels M, Naert I. Image-based planning and clinical validation of zygoma and pterygoid implant placement in patients with severe bone atrophy using customized drill guides. Preliminary results from a prospective clinical follow-up study. Int J Oral Maxillofac Surg. 2003 Feb;32(1):7-14.

17. Bornstein MM, Scarfe WC, Vaughn VM, Jacobs R. Cone beam computed tomography in implant dentistry: a systematic review focusing on guidelines, indications, and radiation dose risks. Int J Oral Maxillofac Implants. 2014;29 Suppl:55-77. doi: 10.11607/jomi.2014suppl.g1.4. PMID: 24660190.

18. Balshi SF, Wolfinger GJ, Balshi TJ. Analysis of 164 titanium oxide-surface implants in completely edentulous arches for fixed prosthesis anchorage using the pterygomaxillary region. Int J Oral Maxillofac Implants. 2005 Nov-Dec;20(6):946-52. PMID: 16392353.

19. Motiwala IA, Bathina T. A Radiographic Study on Pterygoid Implants with Hamulus as a Landmark for Engaging the Pterygoid Plate - A Retrospective Study. Ann Maxillofac Surg. 2022 Jul-Dec;12(2):190-196. doi: 10.4103/ams.ams_132_22. Epub 2023 Jan 10. PMID: 36874784; PMCID: PMC9976848.

20. Holtzclaw D, Telles R. Pterygoid Fixated arch stabilization technique (PFAST): A retrospective study of pterygoid dental implants used for immediately loaded full arch prosthetics. J implant adv clinic dent 2018;10:6 17.

21. Pauwels R, Jacobs R, Singer SR,

Mupparapu M. CBCT-based bone quality assessment: are Hounsfield units applicable? Dentomaxillofac Radiol. 2015;44(1):20140238. doi: 10.1259/dmfr.20140238. PMID: 25315442; PMCID: PMC4277442.
22. Giordano F, D'Ambrosio F, Acerra A, Scognamiglio B, Langone M, Caggiano M. Aumento osseo dopo rialzo del seno mascellare: valutazione a 5 anni della stabilità dell'innesto. J Osseointegration. 2023:221-227. doi: 10.23805/JO.2023.593.
23. Zetehaku Araujo,R., Ferreira Santiago Júnior, J., Lopes Cardoso, C., Froy Benites Condezo,A., Moreira Júnior, R.,Martins Curi, M. Clinical outcomes of pterygoid implants: Systematic review and meta-analysis. J Craniomaxillofac Surg. 2019 47(4):651-660
24. Y.J. Park, S.A. Cho. Retrospective chart analysis on survival rate of fixtures installed at the tuberosity bone for cases with missing unilateral upper molars: a study of 7 cases. J Oral Maxillofac Surg, 68 (2010), pp. 1338-1344
25. Khayat P, Nader N. The use of osseointegrated implants in the maxillary tuberosity. Pract Periodontics Aesthet Dent. 1994 May; 6(4):53-61
26. Graves S.L. The pterygoid plate implant: a solution for restoring the posterior maxilla. Int J Periodontics Restorative Dent. 1994; 14(6):512-23
27. Balshi TJ, Lee HY, Hernandez RE. The use of pterygomaxillary implants in the partially edentulous patient: a preliminary report. Int J Oral Maxillofac Implants. 1995 Jan-Feb; 10(1):89-98.
28. Linkow. The pterygoid extension implant for the totally and partially edentulous maxillae Int J Orthod 1974 Sep;12(3):9-1
29. Linkow, M S Mahler. 3-year report on pterygoid-extension-implants for totally and partially edentulous upper jaws. Oral Implantol. 1975 Jul;2(3):19-29
30. Rodríguez X, Lucas-Taulé E, Elnayef B, Altuna P, Gargallo-Albiol J , Peñarrocha Diago M, Hernandez-Alfaro F. Anatomical and radiological approach to pterygoid implants: a cross-sectional study of 202 cone beam computed tomography examinations. Int. J. Oral Maxillofac. Surg.2016;45:636–640
31. X. Rodriguez, V. Mendez, X. Vela, M. Segala Modified surgical protocol for placing implants in the pterygomaxillary region: clinical and radiologic study of 454 implants Int J Oral Maxillofac Implants, 27 (2012), pp. 1547-1553
32. X. Rodriguez, F. Rambla, L. De Marcos Lopez, V. Mendez, X. Vela, J. Jimenez Garcia. Anatomical study of the pterygomaxillary area for implant placement: cone beam computed tomographic scanning in 100 patientsInt J Oral Maxillofac Implants, 29 (2014), pp. 1049-1052
33. Balshi T.J, Wolfinger G.J., Slauch R.W., Balshi S.F. Brånemark system implant lengths in the pterygomaxillary region: a retrospective comparisonImplant Dent, 22 (2013), pp. 610-612
34. Bidra AS, Peña-Cardelles JF, Iverson M. Implants in the pterygoid region: An updated systematic review of modern roughened surface implants. J Prosthodont. 2023 Apr;32(4):285-291. doi: 10.1111/jopr.13600. Epub 2022 Sep 23. PMID: 36069239.
35. Bidra AS, Sim P, Kuo CL. Survival outcomes of implants placed in the pterygoid region: A retrospective study of up to 9 years. J Prosthodont. 2025 Sep 8. doi: 10.1111/jopr.70031. Epub ahead of print. PMID: 40920120.
36. Uchida Y, Yamashita Y Danjo A, Shibata K, Kuraoka A. Computed tomography and anatomical measurements of critical sites for endosseous implants in the pterygomaxillary region: a cadaveric study. Int J Oral Maxillofac Surg. 2017; 46(6):798-804
37. Giordano F, D'Ambrosio F, Acerra A, Scognamiglio B, Langone M, Caggiano M. Aumento osseo dopo rialzo del seno mascellare: valutazione a 5 anni della stabilità dell'innesto. J Osseointegration. 2023:221-227. doi: 10.23805/JO.2023.593.
38. Suzuki M, Omine Y, Shimoo Y, Yamamoto M, Kaketa A, Kasahara M, Serikawa M, Rhee S, Matsubayashi T, Matsunaga S, Abe S. Regional Anatomical Observation of Morphology of Greater Palatine Canal and Surrounding Structures. Bull Tokyo Dent Coll. 2016;57(4):223-231. doi: 10.2209/tdcpublication.2016-1100. PMID: 28049970.
39. Taniguchi S, Yamamoto M, Tanaka T, Yang T, Watanabe G, Sugiyama Y, Takagi T, Murakami G, Hayashi S, Abe S. Anatomical study of pterygoid implants: artery and nerve passage through bone dehiscence of the greater palatine canal. Int J Implant Dent. 2024 Nov 7;10(1):51. doi: 10.1186/s40729-024-00560-z. PMID: 39508991; PMCID: PMC11543964.
40. Balaji VR, Lambodharan R, Manikandan D, Deenadayalan S. Pterygoid Implant for Atrophic Posterior Maxilla. J Pharm Bioallied Sci. 2017 Nov;9(Suppl 1):S261-S263. doi: 10.4103/jpbs.JPBS_103_17. PMID: 29284976; PMCID: PMC5731027.
41. Salinas-Goodier C, Rojo R, Murillo-González J, Prados-Frutos JC. Three-dimensional descriptive study of the pterygomaxillary region related to pterygoid implants: A retrospective study. Sci Rep. 2019 Nov 7;9(1):16179
42. Jaffin RA, Berman CL. The excessive loss of Branemark fixtures in type IV bone: a 5-year analysis. J Periodontol. 1991 Jan;62(1):2-4. doi: 10.1902/jop.1991.62.1.2. PMID: 2002427.